Stability of a Light Sail Riding on a Laser Beam

Zachary Manchester*
John A. Paulson School of Engineering and Applied Science, Harvard University, 60 Oxford St., Cambridge, MA 02138

Abraham Loeb†
Astronomy Department, Harvard University, 60 Garden St., Cambridge, MA 02138

The stability of a light sail riding on a laser beam is analyzed both analytically and numerically. Conical sails on Gaussian beams, which have been studied in the past, are shown to be unstable in general. A new architecture for a passively stable sail and beam configuration is proposed. The novel spherical shell design for the sail is capable of "beam riding" without the need for active feedback control. Full three-dimensional ray-tracing simulations are performed to verify our analytical results.

arXiv:1609.09506v1 [astro-ph.IM] 29 Sep 2016

I. INTRODUCTION

The light sail concept—harnessing photon pressure to propel a spacecraft—has a long history dating back to some of the earliest pioneers of astronautics. Tsiolkovsky & Zander first described "tremendous mirrors of very thin sheets... using the pressure of sunlight to attain cosmic velocities" in 1925 [1]. Since then, most research has focused on solar sails—light sails that harness solar photons. Following the invention of lasers, in the 1960s Forward [2], Marx [3], and Redding [4] independently proposed the use of high-power lasers as a means of propelling a sail to a significant fraction of the speed of light. This was followed by subsequent studies over the past five decades [5–7]. Most recently, the *Breakthrough Starshot Initiative*[1] was funded to propel a gram-scale spacecraft attached to a sail to a fraction of the speed of light using a high-power laser, with the goal of reaching the nearest stars within several decades.

There are many difficult engineering challenges associated with laser-propelled light sails that remain to be solved. A particularly important problem is ensuring that the sail remains centered on the laser beam despite disturbances, misalignment, and manufacturing imperfections. Ideally, a sail should possess *beam-riding stability* without the need for active feedback control, as the addition of sensor and actuator hardware would add significant complexity and mass to the spacecraft.

While a substantial literature exists on the stability and control of solar sails [8–12], laser-propelled sails have received far less attention. The most closely related previous work has focused on conical microwave-propelled sails, which were studied both in numerical simulations [13, 14] and laboratory experiments [15, 16]. However, a rigorous theoretical analysis of the stability of such sails was not performed.

This paper analyzes the beam-riding stability of laser-propelled light sails and proposes a new passively stable laser and sail configuration. Section II provides an introduction to the beam-riding problem and reviews some basic results from linear stability theory. Next, Section III analyzes the stability of conical sails, which have been studied by several authors [13–16], and shows that they are, in general, unstable. Section IV then proposes a new passively stable spherical sail architecture. Section V presents the results of numerical ray-tracing simulations that demonstrate the stability of the proposed design. Finally, section VI summarizes our results and offers some commentary on future research directions.

II. BACKGROUND

A. The Beam-Riding Problem

The basic features of the beam-riding problem are depicted in Figure 1. A laser beam of width w is incident on a sail of radius r, where w and r are assumed to be of the same order of magnitude. The challenge is—through shaping the sail, choosing its composition, and possibly using active feedback control—to keep the sail centered on the beam as it is accelerated.

The total force applied by a beam incident perpendicular to a perfectly reflective sail of area S is given by,

$$\boldsymbol{F} = \int_S 2\,\frac{P(\boldsymbol{x})}{c}\,\hat{\boldsymbol{n}}(\boldsymbol{x})\,\mathrm{d}S, \tag{1}$$

where the domain of integration is the surface of the sail, $\hat{\boldsymbol{n}}(\boldsymbol{x})$ is the unit vector normal to the sail surface at the point $\boldsymbol{x}$, $P(\boldsymbol{x})$ is the beam power flux at the point $\boldsymbol{x}$, and c is the speed of light. Similarly, the total torque applied by the beam to the sail is given by,

$$\boldsymbol{\tau} = \int_A 2\,\frac{P(\boldsymbol{x})}{c}\,\big(\boldsymbol{r}(\boldsymbol{x}) \times \hat{\boldsymbol{n}}(\boldsymbol{x})\big)\,\mathrm{d}S, \tag{2}$$

where $\boldsymbol{r}(\boldsymbol{x})$ is the vector from the sail's center of mass to point $\boldsymbol{x}$. If the sail is assumed to be rigid, its motion can be described by Newton's second law,

$$m\ddot{\boldsymbol{x}} = \boldsymbol{F}, \tag{3}$$

* zmanchester@seas.harvard.edu
† aloeb@cfa.harvard.edu
[1] http://breakthroughinitiatives.org/concept/3

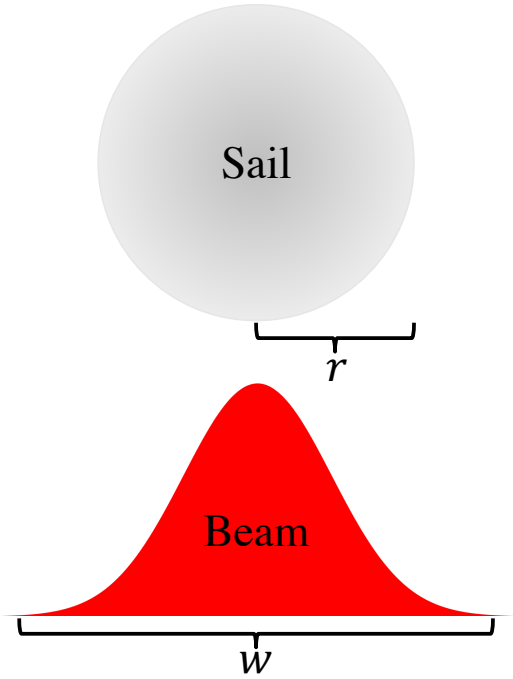

FIG. 1. Schematic illustration of the beam-riding problem.

and Euler's equation,

$$I\dot{\boldsymbol{\omega}} + \boldsymbol{\omega} \times I\boldsymbol{\omega} = \boldsymbol{\tau}, \tag{4}$$

where m is the mass, $\boldsymbol{\omega}$ is the angular velocity vector, and I is the inertia tensor of the sail.

Analyzing the motion of a sail based on equations (1)–(4) is difficult; the integrals in equations (1) and (2) cannot, in general, be computed in closed form, and the differential equation describing angular motion (4) is nonlinear. In the subsequent sections, we will attempt to side-step some of these analytical difficulties to obtain general stability characterizations of various beam-riding configurations.

B. Linear Stability Analysis

We start by briefly reviewing the mathematical formalism of stability theory. For thorough treatments, the reader is referred to references [17] and [18].

A nonlinear dynamical system can be generically written as a first-order vector differential equation,

$$\dot{\boldsymbol{x}} = \boldsymbol{f}(\boldsymbol{x}), \tag{5}$$

where $\boldsymbol{x} \in \mathbb{R}^n$ is the *state vector* of the system. Differential equations involving higher-order derivatives can always be put into this form by introducing additional variables [18]. An *equilibrium point* of the system is a point $\boldsymbol{x}^*$ such that,

$$\boldsymbol{f}(\boldsymbol{x}^*) = 0. \tag{6}$$

Without loss of generality, we will be assume that $\boldsymbol{x}^*$ coincides with the origin.

A linear dynamical system is described by a square matrix $A \in \mathbb{R}^{n\times n}$ such that,

$$\dot{\boldsymbol{x}} = A\boldsymbol{x}. \tag{7}$$

Nonlinear systems can be approximated in the neighborhood of the origin by taking A to be,

$$A_{ij} = \frac{\partial f_i}{\partial x_j}\,. \tag{8}$$

Solutions of (7) are given by,

$$\boldsymbol{x}(t) = e^{At}\boldsymbol{x}_0\,, \tag{9}$$

where $\boldsymbol{x}_0$ is a vector of the initial conditions and e^{At} is a matrix exponential, which is defined in terms of the power series of the exponential function [17].

If A can be decomposed such that $A = VDV^T$, where V is a matrix whose columns are the eigenvectors $\boldsymbol{v}_i \in \mathbb{R}^n$ of A, and D is a diagonal matrix whose entries are the eigenvalues $\lambda_i \in \mathbb{C}$ of A, then equation (9) takes the form,

$$\boldsymbol{x}(t) = Ve^{Dt}V^T\boldsymbol{x}_0 = \sum_{i=1}^{n} V_i e^{t\lambda_i} V_i^T \boldsymbol{x}_0. \tag{10}$$

Equation (10) is simply an expression of the concept of superposition; the solution $\boldsymbol{x}(t)$ is a linear combination of the solutions associated with each eigenvector.

The qualitative stability of the nonlinear system (5) near the origin is characterized by the eigenvalues of A. If all eigenvalues λ_i have a negative real part, then the exponential term in equation (10) will decay to zero as $t \to \infty$ and the state $\boldsymbol{x}(t)$ will tend toward the origin. In such cases, the system is said to be *asymptotically stable*. On the other hand, if one or more eigenvalues have a positive real part, the exponential term in equation (10) will grow unbounded as $t \to \infty$, and the system will be *unstable*. Finally, if the real parts of any λ_i are zero while the rest are strictly negative, the situation is ambiguous and a definitive stability characterization cannot be made based on linearization [18].

III. CONICAL SAILS ON GAUSSIAN LASER BEAMS

Next, we consider the stability of a spinning conical sail riding a Gaussian laser beam, as studied in [13] and [14]. We begin by deriving a simplified linear model that captures the qualitative behavior of the sail about the center of the beam, as depicted in Figure 2. The coordinates x and y are used to describe translation of the sail in the plane orthogonal to the beam and the angles θ and ϕ are used to describe rotation of the sail about the x and y axes, respectively. In addition, we assume that the sail is axially symmetric about the z-axis, with mass m and moments of inertia I_z and $I_x = I_y$, and that it is spinning about the z-axis with angular frequency ω.

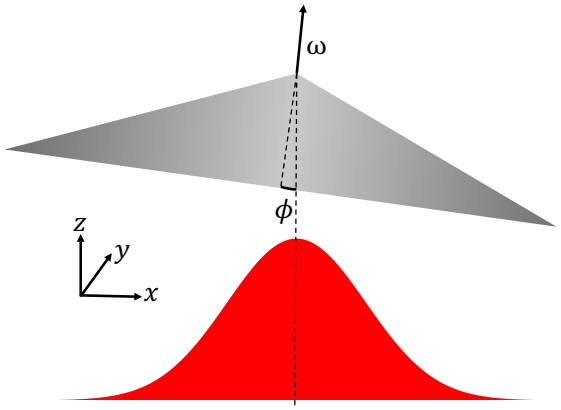

FIG. 2. Schematic illustration of the geometry for a spinning conical sail riding on a Gaussian laser beam.

A. Forces and Torques

Using basic geometry and ray optics, the translational motion of a conical sail near the origin can be approximated by the equations,

$$\begin{aligned} \ddot{x} &= -k_1 x + a_0 \phi \\ \ddot{y} &= -k_1 y - a_0 \theta \end{aligned}, \tag{11}$$

where k_1 is a constant that depends on the sail mass, the cone angle, and the beam shape, and a_0 is the nominal acceleration of the sail in the z direction due to the beam. Equation (11) incorporates both the restoring force due to the sail's conical shape and the forces encountered as the sail tilts, causing a a component of the beam to be deflected in the x-y plane.

The angular motion of the sail near the upright orientation $\theta = \phi = 0$ can be described by,

$$\begin{aligned} \ddot{\theta} &= -k_2 y - k_3 \theta - k_4 \dot{\phi} \\ \ddot{\phi} &= k_2 x - k_3 \phi + k_4 \dot{\theta} \end{aligned}. \tag{12}$$

Equation (12) includes three effects: the torque due to the offset between the beam axis and the sail's center of mass in the x-y plane, a "pendulum torque" due to the separation between the center of pressure and center of mass of the sail along the z-axis, and the gyroscopic effects due to the sail's spin. The constants k_2 and k_3 are given by,

$$k_2 = \frac{a_0 m}{I_x} \quad k_3 = \frac{a_0 m d}{I_x}, \tag{13}$$

where d is the distance between the center of pressure and the center of mass. The constant k_4, which captures the gyroscopic effects, can be derived from Euler's equation (4) by making the assumption that ω is much greater than both $\dot{\theta}$ and $\dot{\phi}$ [19]. Its numerical value is,

$$k_4 = \frac{I_z - I_x}{I_x}\omega. \tag{14}$$

B. Stability

Assembling equations (11) and (12) into the generic form of equation (7) gives the following linear system:

$$\begin{bmatrix} \dot{x} \\ \dot{y} \\ \dot{\theta} \\ \dot{\phi} \\ \ddot{x} \\ \ddot{y} \\ \ddot{\theta} \\ \ddot{\phi} \end{bmatrix} = \begin{bmatrix} 0 & 0 & 0 & 0 & 1 & 0 & 0 & 0 \\ 0 & 0 & 0 & 0 & 0 & 1 & 0 & 0 \\ 0 & 0 & 0 & 0 & 0 & 0 & 1 & 0 \\ 0 & 0 & 0 & 0 & 0 & 0 & 0 & 1 \\ -k_1 & 0 & 0 & a_0 & 0 & 0 & 0 & 0 \\ 0 & -k_1 & -a_0 & 0 & 0 & 0 & 0 & 0 \\ 0 & -k_2 & -k_3 & 0 & 0 & 0 & 0 & -k_4 \\ k_2 & 0 & 0 & -k_3 & 0 & 0 & k_4 & 0 \end{bmatrix} \begin{bmatrix} x \\ y \\ \theta \\ \phi \\ \dot{x} \\ \dot{y} \\ \dot{\theta} \\ \dot{\phi} \end{bmatrix}. \tag{15}$$

Rather than attempting to form the eigen-decomposition of the matrix in (15), which would be quite unwieldy analytically, we instead analyze the growth of a few particular state vectors.

The length of a state vector $\boldsymbol{x}$ using the standard Euclidean norm is,

$$\|\boldsymbol{x}\| = \sqrt{\boldsymbol{x}^T \boldsymbol{x}}. \tag{16}$$

The time derivative of $\|\boldsymbol{x}\|$ can be easily found using the chain rule:

$$\frac{d}{dt}\|\boldsymbol{x}\| = \frac{\boldsymbol{x}^T \dot{\boldsymbol{x}}}{\sqrt{\boldsymbol{x}^T \boldsymbol{x}}} = \frac{\boldsymbol{x}^T A \boldsymbol{x}}{\sqrt{\boldsymbol{x}^T \boldsymbol{x}}} \tag{17}$$

From equation (17), it is clear that if the quadratic form $\boldsymbol{x}^T A \boldsymbol{x}$ is positive, the length of $\boldsymbol{x}$ is increasing. Thus, if any state vector $\boldsymbol{x}$ can be found such that $\boldsymbol{x}^T A \boldsymbol{x} > 0$, the matrix A must have at least one eigenvalue with a positive real part, and the system must be unstable.

We now choose the following state vector,

$$\boldsymbol{x} = \begin{bmatrix} 0 & 0 & 0 & 1 & 1 & 0 & 0 & 0 \end{bmatrix}^T, \tag{18}$$

which corresponds to a sail that is rotated about the y-axis and has some initial velocity in the x direction, and compute $\boldsymbol{x}^T A \boldsymbol{x} = a_0$ using the matrix in (15). Since $a_0 > 0$ by definition, the result is positive, and the system is unstable. This test can be repeated with several other choices of $\boldsymbol{x}$. For example,

$$\boldsymbol{x} = \begin{bmatrix} 0 & 0 & 1 & 0 & 0 & -1 & 0 & 0 \end{bmatrix}^T, \tag{19}$$

which corresponds to a sail that is rotated about the x-axis and has an initial velocity in the $-y$ direction, also results in $\boldsymbol{x}^T A \boldsymbol{x} = a_0$, while

$$\boldsymbol{x} = \begin{bmatrix} 1 & 0 & 0 & 0 & 0 & 0 & 0 & 1 \end{bmatrix}^T \tag{20}$$

and

$$\boldsymbol{x} = \begin{bmatrix} 0 & 1 & 0 & 0 & 0 & 0 & -1 & 0 \end{bmatrix}^T, \tag{21}$$

which correspond to sails that are translated in x or y and have some initial angular velocity, result in $\boldsymbol{x}^T A \boldsymbol{x} = k_2$.

Physically, if the system begins with an initial state vector $\boldsymbol{x}_0$ that has any component along one of these unstable state vectors, that unstable component will grow exponentially, as in equation (10), and the sail will quickly be pushed off the beam. Since small errors are unavoidable in practice, a conical sail would require some form of active feedback control. Any such control system would have to operate at very high frequencies (proportional to a_0), which would be difficult to achieve.

IV. SPHERICAL SHELL DESIGN FOR THE SAIL

We now propose an alternative beam-riding architecture with more favorable stability properties. Upon a closer inspection of the matrix in equation (15), it is clear that the instabilities found in the previous section are rooted in a coupling between the translation and rotation degrees of freedom of the sail. Motivated by this observation, we analyze a spherical shell configuration for the sail, whose symmetry eliminates such coupling.

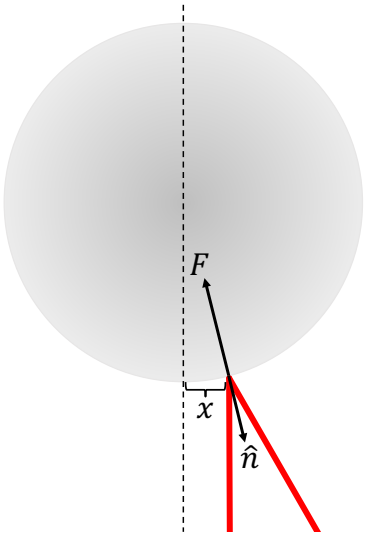

FIG. 3. Schematic illustration of the geometry for a reflective sail in the shape of a thin spherical shell.

Figure 3 depicts the force imparted on a reflective spherical sail by a light ray offset from the center of the sphere. The ray clearly does not produce a restoring force, instead pushing the sphere farther away from the beam axis. Any unimodal beam profile, like the Gaussian studied in the previous section, will have a similar effect, resulting in an unstable system.

If the beam is instead allowed to be multimodal, stable beam riding becomes possible. Figure 4 depicts a beam profile composed of a sum of four Gaussians. An appropriately sized spherical sail perturbed from the center of such a composite beam will experience a restoring force pushing it back toward the center due to the increased power in the sides of the beam. Note that there are no torques applied to the sphere since all forces are directed toward the sphere's center.

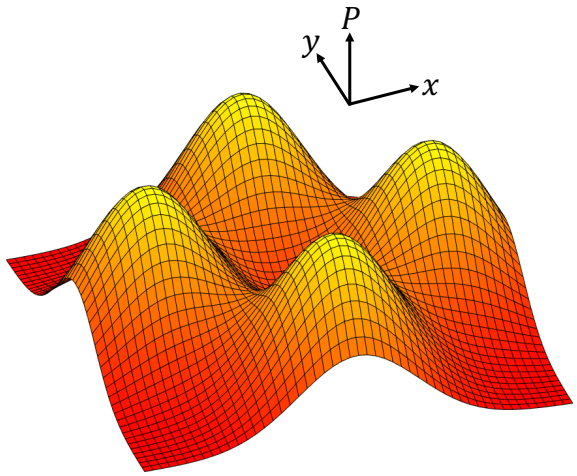

FIG. 4. Multimodal beam profile composed of four Gaussian laser beams.

A linearized model for this beam riding configuration is:

$$\begin{bmatrix} \dot{x} \\ \dot{y} \\ \dot{\theta} \\ \dot{\phi} \\ \ddot{x} \\ \ddot{y} \\ \ddot{\theta} \\ \ddot{\phi} \end{bmatrix} = \begin{bmatrix} 0 & 0 & 0 & 0 & 1 & 0 & 0 & 0 \\ 0 & 0 & 0 & 0 & 0 & 1 & 0 & 0 \\ 0 & 0 & 0 & 0 & 0 & 0 & 1 & 0 \\ 0 & 0 & 0 & 0 & 0 & 0 & 0 & 1 \\ -k_1 & 0 & 0 & 0 & 0 & 0 & 0 & 0 \\ 0 & -k_1 & 0 & 0 & 0 & 0 & 0 & 0 \\ 0 & 0 & 0 & 0 & 0 & 0 & 0 & 0 \\ 0 & 0 & 0 & 0 & 0 & 0 & 0 & 0 \end{bmatrix} \begin{bmatrix} x \\ y \\ \theta \\ \phi \\ \dot{x} \\ \dot{y} \\ \dot{\theta} \\ \dot{\phi} \end{bmatrix}. \tag{22}$$

As expected, there is no coupling between translation and rotation, allowing (22) to be separated into two independent linear systems:

$$\begin{bmatrix} \dot{x} \\ \dot{y} \\ \ddot{x} \\ \ddot{y} \end{bmatrix} = \begin{bmatrix} 0 & 0 & 1 & 0 \\ 0 & 0 & 0 & 1 \\ -k_1 & 0 & 0 & 0 \\ 0 & -k_1 & 0 & 0 \end{bmatrix} \begin{bmatrix} x \\ y \\ \dot{x} \\ \dot{y} \end{bmatrix}, \tag{23}$$

and

$$\begin{bmatrix} \dot{\theta} \\ \dot{\phi} \\ \ddot{\theta} \\ \ddot{\phi} \end{bmatrix} = \begin{bmatrix} 0 & 0 & 1 & 0 \\ 0 & 0 & 0 & 1 \\ 0 & 0 & 0 & 0 \\ 0 & 0 & 0 & 0 \end{bmatrix} \begin{bmatrix} \theta \\ \phi \\ \dot{\theta} \\ \dot{\phi} \end{bmatrix}. \tag{24}$$

Since we are concerned with keeping the sail centered on the beam, we will focus on the translation equations. The eigenvalues of the matrix in equation (23) can be readily found in closed form. Unfortunately, they are $\pm i\sqrt{k_1}$, and do not offer a definitive stability characterization for the full nonlinear system.

To obtain more conclusive stability information, the beam profile of Figure 4 is discretized on a grid and the forces on the sail are evaluated at each grid point. Since

the transverse forces $\boldsymbol{F}_\perp$ depend only on the sail's position in the x-y plane and are not functions of velocity or time, they are conservative [20]. As a result, they can be associated with a scalar potential function $V(x, y)$ such that $\boldsymbol{F}_\perp = -\nabla V(x, y)$. We then compute this potential function numerically, as depicted in Figure 5.

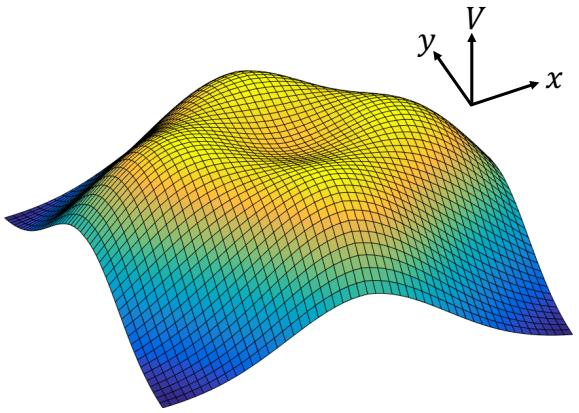

FIG. 5. Potential function $V(x, y)$ for the transverse dynamics of a spherical sail riding on the beam profile shown in Figure 4.

Based on Figure 5, it is clear that there is a basin of attraction surrounding the center of the beam. As long as the sail's initial conditions lie within this basin and its total energy is below the energy associated with the rim of the basin (which can be calculated numerically for any parameters of interest), the sail will remain trapped in the basin. Physically, the sail will oscillate around the center of the beam, but the amplitude of the oscillations will remain bounded and the sail will remain on the beam. While this does not meet the definition of asymptotic stability presented in section II, it does meet the looser requirements of *Lyapunov stability* [21].

V. NUMERICAL SIMULATIONS

We demonstrated the stability of the spherical sail riding on the composite beam profile shown in Figure 4 through two numerical simulations. The integrals in equations (1) and (2) were approximated by discretizing the beam shown in Figure 4 into a grid of 50×50 rays. The path of each ray was then traced as it intersected the sail and reflected off of its surface. The net change in momentum of each ray was calculated, and the resulting forces and torques were applied to the sail. The differential equations (3) and (4) were then integrated forward in time using the standard fourth-order Runge-Kutta method with a time step of 0.001 seconds. The parameters used in our simulations follow the Starshot design, with a beam power $P = 100$ GW, a sail mass $m = 10$ g, a sphere radius $r = 1$ m, a width (full width at half maximum) of each constituent Gaussian in the beam of 1 m, and a distance of 1 m between the center of each constituent Gaussian and the overall beam center.

Figure 6 shows the components of the sail's position vector during a short simulation with an initial offset of 5 cm in both the x and y components of the position vector and zero initial velocity. The sail's position in the x-y plane oscillates with a frequency of roughly 11 Hz but, as predicted, remains bounded.

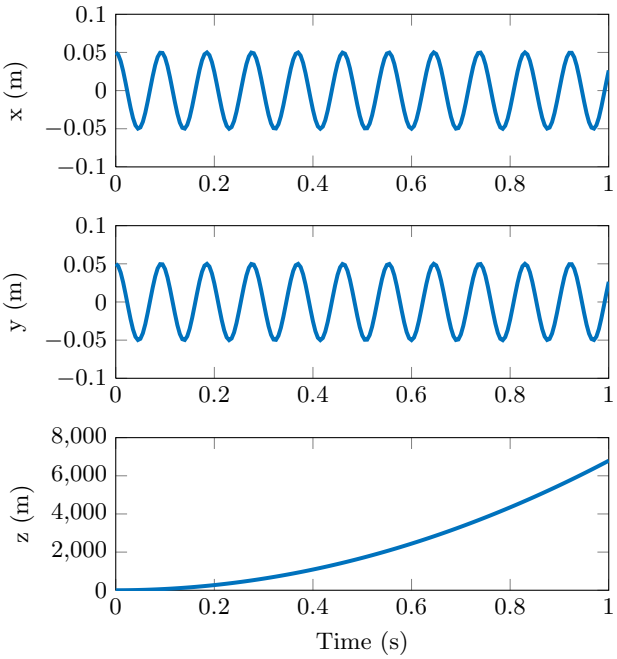

FIG. 6. Sail position during beam-riding simulation.

Figure 7 shows the components of the sail's position vector during a longer simulation in which white noise is added to the rays making up the laser beam to simulate perturbations due to, for example, atmospheric effects. The average power of the noise applied to each ray is chosen to be 10% of that ray's nominal power. While perturbations of the beam clearly excite transverse oscillatory motion of the sail, the sail remains in the stable basin of attraction over a time scale of minutes, which is the time scale needed for it to achieve a sizeable fraction of the speed of light along the z-axis.

In general, noise will add energy to the transverse modes of the system. The total energy of the system will execute a random walk and, after sufficient time, will exceed the energy associated with the rim of the potential well, causing the sail to leave the beam. This "exit time," which depends on the beam power and shape, as well as the power spectral density of the noise, will be an important consideration in the design of a realistic laser-sail system.

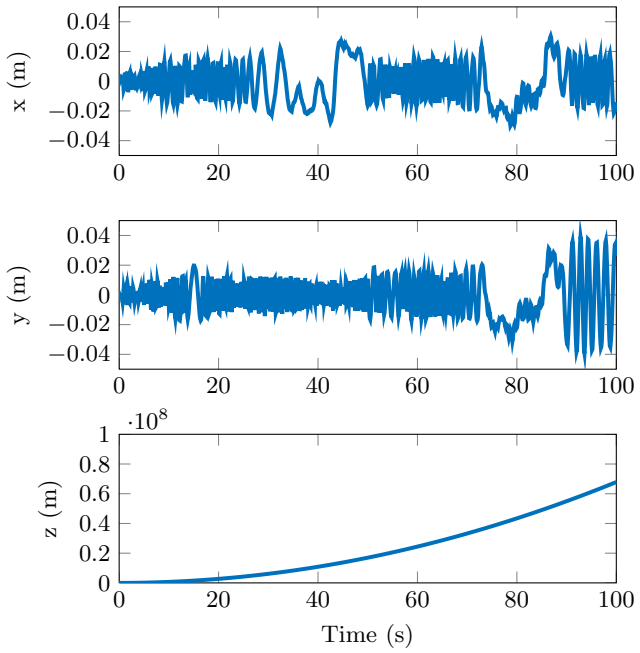

FIG. 7. Sail position during a simulation with white noise of average power equal to 10% of the nominal beam power.

VI. DISCUSSION

We have presented a passively stable laser-sail architecture that is capable of beam riding without active feedback control. The proposed design makes use of a spherical shell sail and a multimodal beam profile. While we have focused on a particular beam profile composed of a sum of four Gaussians, many others are possible, including sums of three or more Gaussians and radially symmetric ring-like profiles.

There are several effects which were not accounted for in this study, but which are likely to be important in the practical implementation of a laser-sail system. Perhaps most importantly, we have assumed a perfectly rigid sail. In practice, the sail will have flexible structural modes which may impact its beam-riding dynamics. Deformation of the sphere's surface could cause non-zero torques on the sail, but could also result in favorable energy damping, which would reduce the amplitude of oscillations about the center of the beam. It may also be possible to pressurize the interior of the sphere with a gas or actively control the structure with actuators to alter both its stiffness and damping properties.

ACKNOWLEDGEMENTS

The authors acknowledge support from the Breakthrough Prize Foundation, and are grateful to the Starshot group at Harvard for comments on the content of this paper.

[1] F. Zander, *Problems of flight by jet propulsion: Interplanetary flights*, NASA Technical Translation F-147 (1964).
[2] R. L. Forward, Journal of Spacecraft and Rockets **21**, 187 (1984).
[3] G. Marx, Nature (London) **211**, 22 (1966).
[4] J. Redding, Nature **213**, 588 (1967).
[5] W. E. Moeckel, Journal of Spacecraft and Rockets **9**, 942 (1972).
[6] R. F. Weiss, A. N. Pirri, and N. H. Kemp, Astronautics and Aeronautics **17**, 50 (1979).
[7] P. Lubin, G. Hughes, J. Bible, and I. Johannson, Journal of the British Interplanetary Society-JBIS (2015).
[8] B. Wie, Journal of Guidance, Control, and Dynamics **27**, 526 (2004).
[9] B. Wie, Journal of Guidance, Control, and Dynamics **27**, 536 (2004).
[10] S. W. Smith, H. Song, J. R. Baker, J. Black, and D. M. Muheim, in *Proceedings of the 46th AIAA/ASME/ASCE/AHS/ASC Structures, Structural Dynamics & Materials Conference, Austin, Texas, American Institute of Aeronautics and Astronautics* (2005).
[11] Y. Mimasu, T. Yamaguchi, M. Matsumoto, M. Nakamiya, R. Funase, and J. Kawaguchi, Advances in Space Research **48**, 1810 (2011).
[12] M. Polites, J. Kalmanson, and D. Mangus, Proceedings of the Institution of Mechanical Engineers, Part G: Journal of Aerospace Engineering **222**, 53 (2008).
[13] E. Chahine, C. Abdallah, D. Georgiev, and E. Schamiloglu, in *AIAA Space 2003 Conference and Exposition* (2003).
[14] E. Schamiloglu, C. T. Abdallah, K. A. Miller, D. Georgiev, J. Benford, G. Benford, and G. Singh, AIP Conference Proceedings **552** (2001).
[15] J. Benford, G. Benford, O. Gornostaeva, E. Garate, M. Anderson, A. Prichard, and H. Harris, AIP Conference Proceedings **608** (2002).
[16] G. Benford, O. Gornostaeva, and J. Benford, AIP Conference Proceedings **664** (2003).
[17] T. Kailath, *Linear Systems*, Information and System Sciences Series (Prentice-Hall, 1980).
[18] M. Hirsch, S. Smale, , and R. Devaney, *Differential Equations, Dynamical Systems, and an Introduction to Chaos*, Pure and Applied Mathematics (Elsevier, 2003).
[19] P. Hughes, *Spacecraft Attitude Dynamics*, Dover Books on Aeronautical Engineering (Dover Publications, Mineola, New York, 2004).
[20] H. Goldstein, C. Poole, and J. Safko, *Classical Mechanics*, 3rd ed. (Addison Wesley, San Francisco, 2001).
[21] H. Khalil, *Nonlinear Systems*, Pearson Education (Prentice Hall, 2002).